

Federated Reinforcement Learning for Uplink Centric Broadband Communication Optimization over Unlicensed Spectrum

Hui Zhou, Yansha Deng, *Senior Member, IEEE*.

Abstract—To provide Uplink Centric Broadband Communication (UCBC), New Radio Unlicensed (NR-U) network has been standardized to exploit the unlicensed spectrum using Listen Before Talk (LBT) scheme to fairly coexist with the incumbent Wireless Fidelity (WiFi) network. Existing access schemes over unlicensed spectrum are required to perform Clear Channel Assessment (CCA) before transmissions, where fixed Energy Detection (ED) thresholds are adopted to identify the channel as idle or busy. However, fixed ED thresholds setting prevents devices from accessing the channel effectively and efficiently, which leads to the hidden node (HN) and exposed node (EN) problems. In this paper, we first develop a centralized double Deep Q-Network (DDQN) algorithm to optimize the uplink system throughput, where the agent is deployed at the central server to dynamically adjust the ED thresholds for NR-U and WiFi networks. Considering that heterogeneous NR-U and WiFi networks, in practice, cannot share the raw data with the central server directly, we then develop a federated DDQN algorithm, where two agents are deployed in the NR-U and WiFi networks, respectively. Our results have shown that the uplink system throughput increases by over 100%, where cell throughput of NR-U network rises by 150%, and cell throughput of WiFi network decreases by 30%. To guarantee the cell throughput of WiFi network, we redesign the reward function to punish the agent when the cell throughput of WiFi network is below the threshold, and our revised design can still provide over 50% uplink system throughput gain.

Index Terms—Federated learning, deep reinforcement learning, NR-U, UCBC, energy detection.

I. INTRODUCTION

With the popularity of emerging data-hungry applications, including high-definition (HD) video surveillance, and unmanned aerial vehicle (UAV) [1], [2], Uplink Centric Broadband Communication (UCBC) has been identified as new service class in the vision of 5.5G to cater for the exponentially growing uplink traffic volume, which leads to a tremendously heavy burden on the existing cellular network due to scarce licensed spectrum and downlink traffic-oriented design [3], [4]. To cope with the ever-increasing uplink traffic demand, the Third Generation Partnership Project (3GPP) has proposed to boost the uplink capacity by exploiting the unlicensed spectrum. In particular, the 3GPP has standardized Long Term Evolution (LTE) based technologies including LTE licensed-assisted access (LTE-LAA) [5], [6] and enhanced LAA (eLAA) [7] to access the unlicensed spectrum since Release 13. Recently, New Radio Unlicensed (NR-U) network

has been standardized to extend the applicability of New Radio (NR) to unlicensed spectrum in Release 16, which determines to support standalone operation mode over unlicensed spectrum [8]–[10].

Although the unlicensed spectrum is a promising solution to provide the cellular network with sufficient uplink spectrum resources, no exclusive rights are granted to any networks in the unlicensed spectrum, which means the NR-U network needs to coexist with the incumbent Wireless Fidelity (WiFi) network [11]. To fairly and harmoniously coexist with the WiFi network, the NR-U network adopts the contention-based access scheme, called Listen Before Talk (LBT), to access the unlicensed spectrum, where the LBT scheme incorporates the Backoff procedure similar to the Carrier-sense multiple access with collision avoidance (CSMA/CA) scheme in WiFi network.

With the goal of improving the throughput over the unlicensed spectrum, the majority of efforts in previous works have been devoted to explicitly optimizing access control parameters using the formulated mathematical model [12]–[14]. The authors in [12] have optimized the transmission time of the LBT scheme with fixed contention window size to maximize the number of devices with guaranteed Quality of Service (QoS), where the combinatorial and nonconvex problem is decomposed into two sub-problems to obtain the sub-optimal solution. In [13], the iterative algorithm has been proposed to optimize the time and power allocation, where devices are assumed to be able to detect each other without HN problem. In [14], the authors have proposed a hybrid duty-cycle and LBT access scheme over the unlicensed spectrum, where the contention window and duty-cycle time fraction are optimized via exhaustive searching method and iterative algorithm, respectively. In [15], [16], the authors derived the optimal initial optimal Backoff window size, where Markov chain was utilized to obtain the successful transmission probability in steady state. However, due to the mathematical complexity of the formulated non-convex problem, all these works optimized the access control parameters with the sub-optimal solution under the impractical assumption for simplicity.

To deal with more complex communication environment and practical formulations, Machine Learning (ML), especially Reinforcement Learning (RL) [17], emerges as a promising tool to optimize access control parameters over the unlicensed spectrum, due to that it solely relies on the self-learning of the environment interaction, without the need to derive explicit optimization solutions based on a complex mathematical model. In [18], each device can be controlled

H. Zhou and Y. Deng are with Department of Engineering, King's College London, London, WC2R 2LS, UK (email:{hui.zhou, yansha.deng}@kcl.ac.uk)(Corresponding author: Yansha Deng).

to transmit or remain silent in every slot based on Deep Reinforcement Learning (DRL) and Federated Learning (FL) approaches, where no NR-U network and HN problem are considered for simplicity. In [19], the authors have proposed to utilize the DRL to optimize the airtime fraction for LTE-LAA without considering the detailed LBT procedures. In [20], a duty-cycle free spectrum sharing framework has been designed, where the DRL algorithm is utilized to maximize the throughput via optimizing the LTE transmission time. In [21], the transmission time of frame-based LBT has been optimized via RL, where each device independently chooses the access technologies, including LTE, LTE-LAA, and WiFi. In [22], RL is combined with FL to optimize the contention window size of WiFi network with the aim to minimize the collision probability. In [23], the authors have proposed to adjust the contention window size with a minimum delay, where the neural network is utilized to predict the number of Negative Acknowledges (NACKs). In [24], the authors proposed a multi-agent RL learning algorithm to optimize the access time and transmission time among Base Stations (BSs), where the mean field technology was utilized to solve the Nash Equilibrium (NE).

However, the above learning-based access control solutions either focused on optimizing the backoff random number or the contention window size in the downlink transmission, without considering the Uplink Centric Broadband Communication (UCBC) over unlicensed spectrum. It is noted that optimizing the contention window size and backoff number fails to solve the hidden node and exposed node problems in the uplink transmission due to the following two reasons: 1) optimizing the contention window and backoff random number only changes the access time of NR-U UEs and WiFi STAs when the collision happens. The devices with fixed energy detection threshold will continue to identify the channel as idle and transmit data when the channel is occupied by other devices for a long time, which may still lead to collision; 2) each UE maintains a different contention window size and backoff number independently in the uplink transmission, which means optimizing the contention window size and backoff number in the uplink transmission requires much higher number of agents (i.e., proportional to the number of the UEs) than the downlink (i.e., proportional to the number of BSs). Therefore, we propose federated reinforcement learning algorithm to dynamically optimize the common energy detection threshold adopted by all UEs. Furthermore, the existing works merely evaluated system throughput to indicate the network-centric performance, and ignored the user-centric Quality of Experience (QoE) [25], [26], which is more intuitive to reveal individual user experience in the UCBC.

In this article, we address the following fundamental questions: 1) how to optimize the uplink system throughput over unlicensed spectrum under the coexistence of heterogeneous networks; 2) how to guarantee the fairness between heterogeneous networks during optimization; 3) how to evaluate the effectiveness of proposed algorithm in improving the user-centric QoE performance. To do so, we develop DRL-based ED thresholds configuration approaches to dynamically optimize the uplink system throughput under the coexistence

of NR-U and WiFi networks. Our contributions can be summarized as follows:

- We develop a DRL-based framework to optimize the uplink system throughput by adaptively configuring the ED thresholds under the coexistence of heterogeneous NR-U and WiFi networks. In the framework, the uplink transmission procedure over the unlicensed spectrum is simulated by taking into account the traffic characteristic of UCBC, the process of LBT and CSMA/CA access schemes, uplink transmission scheduling in NR-U network, and the collision among devices, which is used for training the DRL-based agent before deployment.
- We first propose a centralized double Deep Q-Network (DDQN) algorithm to optimize the uplink system throughput via dynamically configuring the ED thresholds for both the NR-U and WiFi networks, where the agent is deployed at the central server to observe the number of successfully transmitted packets of both networks during training and testing phase in real-time. Two different NR-U uplink transmission procedures are considered according to the 3GPP standard [27], where the UE can either perform Category (Cat) 2 LBT or Cat4 LBT to transmit the packet.
- To protect the data privacy of the NR-U and WiFi networks, we then develop a federated DDQN algorithm via Federated Averaging (FedAve), where two agents are deployed at the NR-U and WiFi networks, respectively. Two agents exchange the model parameters with the central server, and can be independently deployed in NR-U and WiFi networks during the testing phase [28]. It is noted that we introduce the user-centric performance metric, user perceived throughput (UPT), to evaluate the file transmission throughput improvement from the perspective of users.
- As the NR-U network has inherent advantages over the WiFi network, including higher data rate and scheduling procedure, the agent tends to sacrifice the cell throughput of WiFi network for higher uplink system throughput under the coexistence scenario. In order to take the fairness into account, we redesign the reward function to guarantee the cell throughput of WiFi network, where the agent gets punished when the cell throughput of WiFi network is lower than the pre-defined threshold.
- Finally, our proposed DRL-based learning framework is evaluated to optimize the uplink system throughput in heterogeneous NR-U and WiFi networks. Without considering the fairness, the results have shown that the system throughput achieves up to 100% performance gain, where the cell throughput of NR-U network increases by 150%, and the cell throughput of WiFi network decreases by 30%. Taking the fairness into account, our results, the results have shown that the cell throughput of WiFi network is even higher than the benchmark scheme with fixed ED thresholds, where the system throughput achieves 70% performance gain under File Transfer Protocol 3 (FTP-3) traffic, and 50% performance gain under more dynamic Beta traffic. In terms of the UPT, the performance gain

of NR-U network achieves over 100% in all experimental settings.

The remainder of this paper is organized as follows. Section II provides the system model of the NR-U and WiFi networks. Section III describes the problem analysis and formulation. Section IV elaborates the proposed centralized DRL and federated DRL algorithms for solving the formulated problem. Section V illustrates the numerical results. Finally, Section VI concludes the paper.

II. SYSTEM MODEL

We consider the uplink transmission of the 3GPP indoor scenario as shown in Fig. 1, where NR-U and WiFi networks deploy three small cells in a one-floor building, respectively [27]. It is noted that the heterogeneous NR-U and WiFi networks share a single 20-MHz unlicensed channel for transmission. The set of WiFi stations (STAs) and NR-U User Equipments (UEs) are denoted by \mathcal{W} and \mathcal{U} , respectively. The set of access points (APs) and gNodeBs (gNBs) are denoted by \mathcal{P} and \mathcal{G} , respectively. We assume that STAs and UEs are uniformly distributed in the scenario, where each STA or UE is connected to the closest AP or gNB. The main notations are summarized in Table I.

TABLE I
NOTATION TABLE

Notations	Physical means
S_{file}	File Size
T_{con}	Time Constraint
CW_{max}	Maximum Contention Window
CW_{min}	Minimum Contention Window
N	Backoff Number
λ	Packet Arrival Rate
$P_{\{S,U\}}$	Transmit Power of UE and STA
$P_{\{G\}}$	Transmit Power of gNB
σ_n^2	Noise Power
h	Channel Power Gain
α	Transmission Indicator
\mathcal{I}	Interference
η_w	WiFi SINR Threshold
η_n	NRU SINR Threshold
λ_w^{CS}	WiFi Preamble Detection Threshold
λ_w^{ED}	WiFi Energy Detection Threshold
λ_n^{ED}	NRU Energy Detection Threshold

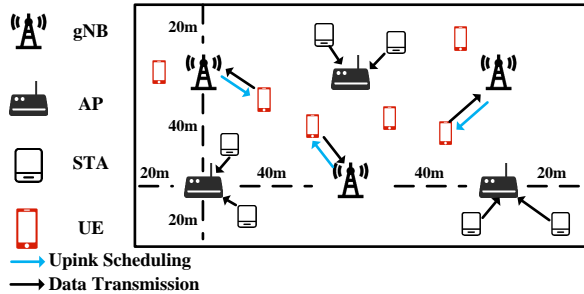


Fig. 1. Uplink transmission of NR-U and WiFi indoor coexistence scenario.

A. Network and Traffic Model

We consider a flat Rayleigh small-scale fading channel, where the channel power gains $\beta(x, y)$ between two generic locations $x, y \in \mathbb{R}^3$ is assumed to be exponentially distributed random variables with unit mean. All the channel gains are independent of each other, independent of the spatial locations, and identically distributed (i.i.d.).

The indoor mixed office path-loss model is adopted as [29]

$$\zeta_L(x, y) = 32.4 + 17.3 \log_{10}(d_{3D}) + 20 \log_{10}(f_c), \quad (1)$$

$$\zeta_N(x, y) = 32.4 + 31.9 \log_{10}(d_{3D}) + 20 \log_{10}(f_c), \quad (2)$$

where $\zeta_L(x, y)$ and $\zeta_N(x, y)$ represent the pathloss under line-of-sight (LoS) and non line-of-sight (NLoS), f_c is the carrier frequency, and d_{3D} is the distance between two locations x and y . The indoor mixed office LoS probability P_{LoS} is given as

$$P_{\text{LoS}} = \begin{cases} 1 & , d_{2D} < 1.2\text{m} \\ \exp\left(\frac{d_{2D} - 1.2}{4.7}\right) & , 1.2\text{m} \leq d_{2D} \leq 6.5\text{m} \\ \exp\left(\frac{d_{2D} - 6.5}{32.6}\right) & , d_{2D} > 6.5\text{m} \end{cases} \quad (3)$$

where d_{2D} is the projection of d_{3D} on the horizontal plane. Accordingly, the NLoS probability P_{NLoS} is

$$P_{\text{NLoS}} = 1 - P_{\text{LoS}}. \quad (4)$$

Therefore, the mean channel power gain is derived as

$$h = (10^{-\zeta_L/10} P_{\text{LoS}} + 10^{-\zeta_N/10} P_{\text{NLoS}}) \beta, \quad (5)$$

where the spatial indices (x, y) are dropped for the brevity of exposition.

To capture the burst traffic characteristic of UCBC, we consider the FTP-3 traffic model for each STA and UE with fixed size S_{file} , where packets arrive according to a Poisson process with arrival rate λ [30], [31]. Without loss of generality, First Come First Serve (FCFS) scheduling scheme is applied by placing the newly arrived packets at the end of the queue. We assume each packet has a time constraint T_{con} , where the packet is dropped if it is not successfully transmitted within the time constraint.

B. Channel Access Schemes in Unlicensed Band

As heterogeneous WiFi and NR-U networks coexist over the unlicensed spectrum with different access schemes, we present the detailed procedures of the CSMA/CA and LBT access schemes in this section, respectively.

1) *Carrier-Sense Multiple Access with Collision Avoidance*: The WiFi network adopts the CSMA/CA to access the unlicensed spectrum [32], also known as distributed coordination function (DCF), which integrates the Backoff procedure as shown in Fig. 2 (a). When the new packet arrives, the STA is required to perform CCA to determine whether the channel is busy or idle. If the channel has been continuously idle over a DCF inter-frame space (DIFS) interval, it transmits the packet immediately. Otherwise, the STA defers its transmission until the channel becomes idle. Then if the channel is detected to be continuously idle over a DIFS interval, the STA will initiate

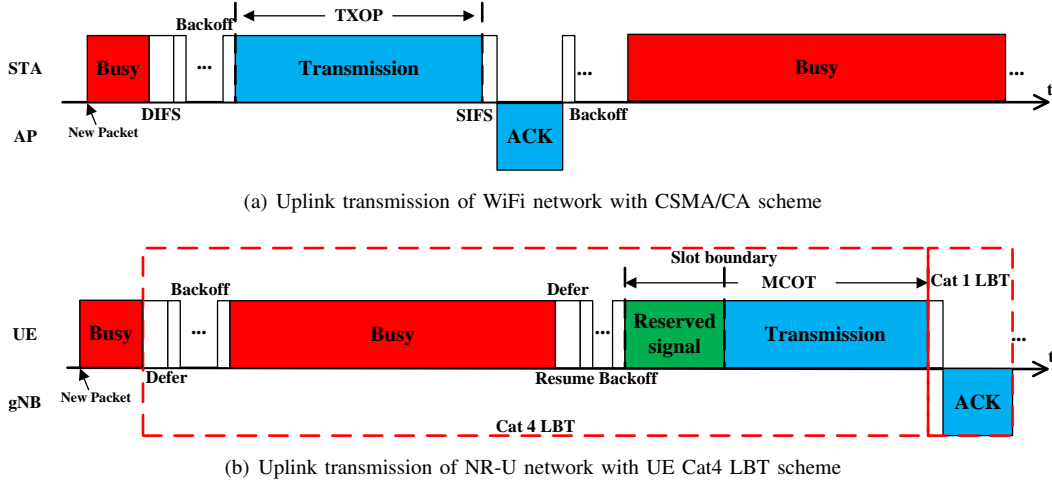


Fig. 2. Timing graph of uplink transmission for WiFi and NR-U networks.

the Backoff procedure to further defer its transmission over a random time interval. The back-off procedure starts with the selection of an integer N , where N is a random number uniformly distributed in the range from 0 to the contention window CW . It is noted that the CW is initialized to be the minimum value CW_{\min} . Next, the generated random number N decreases when the CCA identifies the channel to be idle. Otherwise, the random number N is frozen, and continues to decrease when the CCA identifies the channel to be idle again within a DIFS interval. Once N reaches zero, the STA transmits its data within the transmission opportunity (TXOP). It is important to note that this Backoff procedure randomizes the channel access among STAs and thus helps to reduce the chance of collision.

Upon receiving the packet correctly, the AP waits for a Short inter-frame space (SIFS) interval, and transmits an ACK back to the STA to confirm the correct reception. When the transmission is successful, the contention window CW is reset to its minimum value CW_{\min} . Otherwise, the STA activates the retransmission procedure for the lost packet, where the contention window size CW is doubled until it reaches a maximum value CW_{\max} .

2) *Listen Before Talk*: To fairly share the unlicensed spectrum with the incumbent WiFi network, the NR-U network has agreed to adopt the LBT schemes, which consist of following three categories:

- Cat4: LBT with random Backoff and a contention window of variable size,
- Cat2: LBT without random Backoff,
- Cat1: Immediate transmission after a short switching gap.

As shown in Fig. 2 (b), the UE adopts the Cat4 LBT channel access scheme to transmit the user data using the scheduled Physical Uplink Shared Channel (PUSCH) resource. Inheriting the Backoff procedure from CSMA/CA, the UE is required to perform CCA to check whether the channel has been continuously idle over a Defer interval when the new packet arrives. If the channel has been idle for a Defer interval, it transmits immediately. Otherwise, the UE defers its transmission until the channel becomes idle. Once the channel

is detected to be continuously idle over a Defer interval, the UE will initiate the Backoff procedure to further defer its transmission over a random time interval as CSMA/CA. Once the random number N finally reaches zero, the UE can transmit its data within the maximum channel occupancy time (MCOT). It is noted that the UE can only start data transmission at the spectrum slot boundary (SSB). Hence, if the Backoff procedure does not end at the SSB, the UE is required to transmit a reserved signal (RS) until the SSB.

Although the Backoff procedure reduces the collision probability, it also leads to additional controlling overheads. Therefore, 3GPP determines to support the Cat2 LBT channel access scheme, which only needs to guarantee the channel to be idle for $25\mu s$ continuously before transmission without Backoff procedure.

The Cat1 LBT channel access scheme is referred to as “no LBT”. More specifically, if the gap between two successive transmissions is less than or equal to $16\mu s$, the latter transmission does not need to perform any LBT. As shown in Fig. 2 (b), Cat 1 LBT is beneficial for NR-U to support fast ACK/NACK feedback transmission, where the gap between PUSCH and Physical Downlink Control Channel (PDCCH) is less or equal to $16\mu s$.

C. Key Differences between NR-U and WiFi Networks

Although the Cat4 LBT access schemes adopt similar procedures as CSMA/CA to guarantee the fairness, there are fundamental differences between the WiFi and NR-U networks in terms of the frame structure, uplink scheduling, and access category, which are presented in detail in this section.

1) *Frame Structures*: As we mentioned above, the WiFi STA can start the data transmission once the random number N decreases to zero. However, the NR-U UE can only start the data transmission at the exact SSB, which can hardly be guaranteed due to the random nature of Backoff procedure [33]. Currently, 3GPP has not explicitly defined the behaviour between the end of Backoff and SSB. Considering that if the NR-U UE decides to wait for the SSB without transmission, WiFi STAs may identify the channel as idle and occupy the

channel, which leads to poor NR-U network performance. Therefore, it is usually suggested to send an RS to occupy the channel until the SSB [34].

However, the transmission of RS introduces the controlling overheads, especially with larger slot length (e.g., with a period $\theta = 500\mu s$ in the LTE-LAA network). It is noted that the problem can be alleviated in NR-U network based on its flexible radio numerology, where the NR-U network adopts higher subcarrier spacing (SCS), and even mini-slot to reduce the slot length and RS overheads [35].

2) *Uplink Transmission Procedure*: In the WiFi network, each STA performs the CSMA/CA to access the unlicensed channel once the new packets arrive, where the AP does not schedule the STA to transmit. Each WiFi STA accesses the channel independently, and transmits the uplink user data once it obtains the channel. However, in each NR-U cell, NR-U UEs are scheduled for uplink transmission in a centralized way, where each UE needs to be scheduled individually before transmitting the user data using the granted PUSCH resource. Therefore, there is only inter-cell interference between the NR-U UEs without intra-cell interference.

The 3GPP standard has identified uplink transmission procedure as shown in the Fig. 3, where the gNB is required to perform the Cat4 LBT to schedule the UE via PDCCH. Then the UE can either perform Cat2 LBT as Fig. 3(a) or Cat4 LBT as Fig. 3(b) to transmit the user data on the granted PUSCH resource [27]. For simplicity, these two uplink transmission schemes are termed as gNB-Cat4/UE-Cat2 and gNB-Cat4/UE-Cat4, respectively. It is noted that when the UE performs the Cat2 LBT, the UE can access the channel after Defer time without performing Backoff procedure, which can be adopted for latency-sensitive service to guarantee the stringent latency requirement.

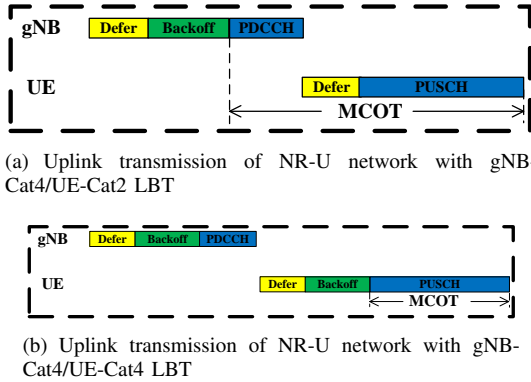


Fig. 3. Procedures of gNB scheduling and UE data transmission.

3) *Access Category*: As the basic DCF with CSMA/CA scheme lacks capabilities to guarantee the QoS of different applications, the enhanced distribution coordination function (EDCF) has introduced the concept of access category (AC), where four priority levels are defined to differentiate the channel access probability for different traffic types [36]. Correspondingly, the LBT access schemes also define four priority levels with different parameters, where shorter wait time and contention window size correspond to higher priority service [37].

III. PROBLEM ANALYSIS AND FORMULATION

To capture the characteristics of uplink transmission with CSMA/CA and LBT access schemes over unlicensed spectrum, we consider the Carrier Sensing (CS) & ED, and Signal to Interference Plus Noise Ratio (SINR) to model the CCA and data transmission, respectively, which are then utilized to formulate the system throughput optimization problem under the WiFi and NR-U coexistence scenario. We also introduce a performance metric called UPT to evaluate the user-centric QoE.

A. Carrier Sensing & Energy Detection

In WiFi network, each STA is required to perform CCA during the DIFS interval and Backoff procedure to determine whether the channel is busy or idle in each slot. The CCA in WiFi network consists of the CS & ED, where the CS detects the preamble transmission of WiFi network, and ED detects the total energy on the channel including both transmissions from NR-U and WiFi networks. We formulate the CS and ED of WiFi STA i ($i \in \mathcal{W}$) as

$$\text{WiFi}_i^{\text{CS}} = \sum_{w \in \mathcal{W} \setminus i} \alpha_w P_w h_{w,i}, \quad (6)$$

$$\text{WiFi}_i^{\text{ED}} = \sum_{w \in \mathcal{W} \setminus i} \alpha_w P_w h_{w,i} + \sum_{u \in \mathcal{U}} \alpha_u P_u h_{u,i} + \sum_{g \in \mathcal{G}} \alpha_g P_g h_{g,i}, \quad (7)$$

where $w \in \mathcal{W}$ denotes the STA, $u \in \mathcal{U}$ denotes the UE, $g \in \mathcal{G}$ denotes the gNB. In (6) and (7), $\alpha_{\{w,u,g\}}$ indicates whether device $\{w,u,g\}$ is transmitting or not, $h_{\{w,u,g\},i}$ is the channel gain between device $\{w,u,g\}$ and STA i , and $P_{\{w,u,g\}}$ is the transmit power.

As shown in (6) and (7), the STA only senses the transmission of other STAs in the CS, but detects the transmission energy of all other devices in the ED. The STA will only identify the channel as idle when the values of CS and ED are under the pre-defined threshold $\lambda_w^{\text{CS}} = -82\text{dBm}$ and $\lambda_w^{\text{ED}} = -62\text{dBm}$, respectively.

In the NR-U network, the NR-U device $i \in \mathcal{U} \cup \mathcal{G}$ is required to perform CCA during the Defer interval and Backoff procedure to determine whether the channel is busy or idle in each slot, which is formulated as

$$\text{NR}_i^{\text{ED}} = \sum_{w \in \mathcal{W}} \alpha_w P_w h_{w,i} + \sum_{u \in \mathcal{U} \setminus i} \alpha_u P_u h_{u,i} + \sum_{g \in \mathcal{G} \setminus i} \alpha_g P_g h_{g,i}. \quad (8)$$

When the ED is below the predefined threshold $\lambda_n^{\text{ED}} = -72\text{dBm}$, the channel is identified as idle.

B. Signal to Interference Plus Noise Ratio

The device starts the transmission once finishing the Backoff in WiFi network or at the exact SSB in NR-U network. However, due to the interference from the hidden nodes or channel fading, the receiver may fail to decode the transmitted signal. We model the decoding process via the SINR, where the SINR of data transmission from device $i \in \mathcal{K}$ to the device $j \in \mathcal{K}$ can be represented as

$$\text{SINR}_{i,j} = \frac{P_i h_{i,j}}{\sum_{k \in \mathcal{K} \setminus i} \alpha_{k,i} P_k h_{k,j} + \sigma_n^2}, \quad (9)$$

where $\mathcal{K} = \mathcal{W} \cup \mathcal{U} \cup \mathcal{G} \cup \mathcal{P}$ represents the set of all devices, α_k indicates whether device k is transmitting or not, $h_{i,j}$ is the channel from device i to the device j , P_i represents the transmit power of device i , and σ_n^2 is the power of the noise.

C. User Perceived Throughput

Since the system throughput can only reflect the network-level performance, we introduce a user-centric performance metric called UPT to evaluate the file transmission throughput from the perspective of users. The UPT is obtained by averaging all file throughputs [31], where each file throughput T_{file} is calculated as

$$T_{\text{file}} = \begin{cases} \frac{S_{\text{file}}}{T_{\text{departure}} - T_{\text{arrival}}} & , \text{Transmitted File} \\ \frac{S_{\text{served}}}{T_{\text{end}} - T_{\text{arrival}}} & , \text{Unfinished File} \\ 0 & , \text{Dropped File} \end{cases} \quad (10)$$

where S_{file} is the file size, S_{served} is the transmitted file size by the end of simulation, T_{arrival} is the arrival time of the file, and $T_{\text{departure}}$ represents the transmitted time of the file. It is noted that the file throughput is zero when the file is dropped due to time violation.

D. Hidden Node and Exposed Node Problem

As the devices contend for the unlicensed spectrum without coordination, in both NR-U and WiFi networks, each device is required to perform Clear Channel Assessment (CCA) to sense the ongoing transmissions over the channel before its own transmission, where the sensed energy is compared with the fixed Energy Detection (ED) threshold to determine whether the channel is idle or busy. In other words, each device can only transmit when the channel is detected to be idle. However, the CCA procedure based on the fixed ED threshold cannot fully mitigate the throughput degradation due to the lack of coordination function among devices, which leads to the hidden node (HN) problem and exposed node (EN) problem [38].

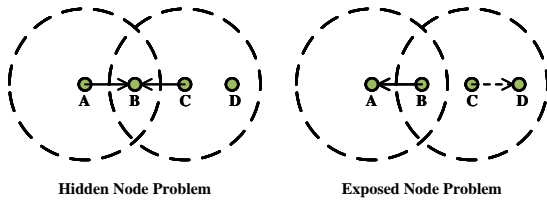


Fig. 4. Hidden node problem and exposed node problem.

As shown in the Fig. 4, the HN problem happens when transmitter A and transmitter C cannot sense the transmission of each other (i.e., the sensed energy is lower than the ED threshold) due to the pathloss and fading. Hence, two transmitters will send the packets simultaneously, which causes strong co-channel interference and transmission failure at receiver B. The EN problem happens when the transmitter C is prevented from sending packet to receiver D because of co-channel interference from the neighboring transmitter B (i.e.,

the sensed energy is higher than the ED threshold). However, receiver D could still receive the transmission from C with low interference because receiver D is far away from transmitter B, which leads to low spectral efficiency. Moreover, NR-U and WiFi networks adopt asymmetry ED thresholds (e.g., -72dBm in NR-U network and -62dBm in WiFi network), which makes the HN and EN problems even worse [39]. In a word, the high ED threshold setting enables multiple devices to transmit simultaneously, but may lead to stronger interference. On the contrary, the low ED threshold setting mitigates the probability of collision, but leads to low spectrum efficiency [40].

E. Uplink System Throughput Optimization

As discussed above, the WiFi STAs perform CSMA/CA individually to access the channel without scheduling, and all the STAs that accessed the channel would transmit in a grant-free manner. The gNB is required to perform the Cat4 LBT to access the channel, and transmits the scheduling information via the PDCCH. Then, the scheduled UE is required to perform Cat2 or Cat4 LBT to transmit the user data based on its scheduled resource. In this work, we tackle the problem of optimizing the coexistence of NR-U and WiFi configuration defined by action parameters $A^t = \{\lambda_w^{\text{ED},t}, \lambda_n^{\text{ED},t}\}$ for WiFi and NR-U networks in each transmission time interval (TTI) t , where $\lambda_w^{\text{ED},t}$ and $\lambda_n^{\text{ED},t}$ represent the ED threshold for NR-U and WiFi networks, respectively.

In order to select the action at the beginning of every TTI t , the central server accesses all prior historical observations $U^{t'}$ in TTIs $t' = 1, \dots, t-1$ consisting of the following variables: the number of successfully transmitted WiFi packets $N_w^{t'}$, and the number of successfully transmitted NR-U packets $N_n^{t'}$. We denote $O^t = \{A^{t-1}, U^{t-1}, A^{t-2}, U^{t-2}, \dots, A^1, U^1\}$ as the observed history of all such measurements and past actions.

The WiFi and NR-U networks aim at maximizing the long-term average system throughput with respect to the stochastic policy π that maps the current observation history O^t to the probabilities of selecting each possible configuration A^t . This problem can be formulated as

$$(P1): \quad \max_{\{\pi(A^t|O^t)\}} \sum_{k=t}^{\infty} \gamma^{(k-t)} \mathbb{E}_{\pi}[(N_w^k + N_n^k) \times S_{\text{file}}], \quad (11)$$

where $\gamma \in [0, 1)$ is the discount rate for the performance in future TTIs, and S_{file} is the file size. Since the dynamics of the system is Markovian over the TTIs, this is a partially observable Markov decision process (POMDP) problem that is generally intractable. Approximate centralized and federated solutions will be discussed in Section IV-A and Section IV-B, respectively.

IV. UPLINK SYSTEM THROUGHPUT OPTIMIZATION BASED ON DEEP REINFORCEMENT LEARNING

DRL is one of the most promising solutions to optimally solve complex POMDP problems, due to the reliance on the deep neural networks as one of the most powerful non-linear approximation functions [41]. The related DRL algorithms have been widely used in the dynamic optimization

for wireless communication systems, e.g., [42]–[44]. However, they have been rarely studied in handling the ED thresholds configuration under the coexistence of heterogeneous NR-U and WiFi networks. Therefore, we design the centralized DRL and federated DRL in this section to evaluate the capability of DRL algorithm, respectively.

A. Centralized Deep Reinforcement Learning

In the central server, an agent is deployed to optimize the system throughput of the NR-U and WiFi networks, the agent is required to explore the environment in order to choose appropriate actions progressively leading to the optimization goal. We define $s \in \mathcal{S}$, $a \in \mathcal{A}$, and $r \in \mathcal{R}$ as any state action, and reward from the their corresponding sets, respectively. At the beginning of the t th TTI ($t \in \{0, 1, 2, \dots\}$), the agent first observes the current state S^t corresponding to a set of previous observations ($O^t = \{U^{t-1}, U^{t-2}, \dots, U^1\}$) in order to select an specific action $A^t \in \mathcal{A}(S^t)$. The action A^t is designed to be the WiFi and NR-U ED thresholds $\lambda_w^{\text{ED},t}, \lambda_n^{\text{ED},t}$, respectively.

We consider a basic state function under the coexistence of NR-U and WiFi networks, where S^t is a set of indices mapping to the current observed information $U^{t-1} = [N_w^{t-1}, N_n^{t-1}]$. With the knowledge of the state S^t , the agent chooses an action A^t from the set \mathcal{A} , which is a set of indices mapped to the set of available ED thresholds \mathcal{F}_{ED} . Once an action A^t is performed, the agent will receive a scalar reward R^{t+1} , and observe a new state S^{t+1} . The reward R^{t+1} indicates to what extent the executed action A^t can achieve the optimization goal, which is determined by the new observed state S^{t+1} . As the optimization goal is to maximize the system throughput of NR-U and WiFi networks, we define the reward R^{t+1} as the size of transmitted data packets in each TTI

$$R^{t+1} = (N_w^t + N_n^t) * S_{\text{file}}. \quad (12)$$

where S_{file} is the size of each packet, N_w^{t-1} is number of successfully transmitted packets in the WiFi network, and N_n^{t-1} is number of successfully transmitted packets in the NR-U network.

The basic Q-learning is a value-based RL approach, where the policy of states to actions mapping $\pi(s) = a$ is learned using a state-action value function $Q(s, a)$ to determine an action for the state s . In the Q-learning, a lookup table is utilized to represent the state-action value function $Q(s, a)$, which consists of value scalars for all the state and action spaces. To obtain an action A^t , the highest value scalar is selected from the numerical value vector $Q(S^t, a)$, which maps all possible actions under S^t to the Q-value table $Q(s, a)$.

Accordingly, the objective is to find an optimal Q-value table $Q^*(s, a)$ with optimal policy π^* that can select actions to dynamically optimize the system throughput of NR-U and WiFi networks. To do so, an initial Q-value table $Q(s, a)$ is trained in the environment, where $Q(s, a)$ is immediately updated using the current observed reward R^{t+1} after each action as

$$Q(S^t, A^t) = Q(S^t, A^t) + \eta \left[R^{t+1} + \gamma \max_{a \in \mathcal{A}} Q(S^{t+1}, a) - Q(S^t, A^t) \right], \quad (13)$$

where η is a constant step-size learning rate that affects how fast the algorithm adopts to a new environment, $\gamma \in [0, 1)$ is the discount rate that determines how current rewards affects the value function updating $\max_{a \in \mathcal{A}} Q(S^{t+1}, a)$ approximates the value in optimal Q-value table $Q^*(s, a)$ via the up-to-date Q-value table $Q(s, a)$ and the obtained new state S^{t+1} .

Specifically, the learning rate η is suggested to be set to a small number (e.g., $\eta = 0.01$) to guarantee the stable convergence of Q-value table under the coexistence of NR-U and WiFi networks. This is due to that a single reward in a specific TTI can be severely biased, because state function is composed of multiple unobserved information with unpredictable distributions.

However, Q-learning needs each element to be updated to converge, searching for an optimal policy can be difficult with limited time and computational resources. To solve this problem, we use a value function approximator instead of Q-value table to find a sub-optimal approximated policy. We conduct the DNN for Q-learning as a more effective but complicated function approximator, which is also known as DQN. As shown in the Fig. 5, the DQN agent parameterizes the action-state value function $Q(s, a)$ by using a function $Q(s, a; \theta)$, where θ represents the weights matrix of a DNN with multiple layers. In the learner, the weights θ is updated through Stochastic gradient descent (SGD) based on the mini-batch sample. In the actor, the action is determined based on the ϵ -greedy approach. We consider the conventional DNN, where neurons between two adjacent layers are fully pairwise connected, namely fully-connected layers. The input of the DNN is given by the variables in state S^t ; the intermediate hidden layers are Rectifier Linear Units (ReLU) by using the function $f(x) = \max(0, x)$; while the output layer is composed of linear units, which are in one-to-one correspondence with all available actions in \mathcal{A} .

We consider ϵ -greedy approach to balance exploitation and exploration in the Actor of the Agent, where ϵ is a positive real number and $\epsilon \leq 1$. In each TTI t , the agent randomly generates a probability p_ϵ^t to compare with ϵ . Then, with the probability ϵ , the algorithm randomly chooses an action from the remaining feasible actions to improve the estimate of the non-greedy action's value. With the probability $1 - \epsilon$, the exploitation is obtained by performing forward propagation of Q-function $Q(s, a; \theta)$ with respect to the observed state S^t , which can be calculated as follows:

$$a = \begin{cases} \max_{a \in \mathcal{A}} Q(S^{t+1}, a; \bar{\theta}^t) & , \text{ with probability } 1 - \epsilon \\ \text{Random action} & , \text{ with probability } \epsilon. \end{cases} \quad (14)$$

The weights matrix θ is updated online along each training episode by using double deep Q-learning (DDQN), which to some extent reduce the substantial overestimations of value function. Accordingly, learning takes place over multiple training episodes, with each episode of duration N_{TTI} TTI periods. In each TTI, the parameter θ of the Q-function approximator $Q(s, a; \theta)$ is updated using RMSProp optimizer as

$$\theta^{t+1} = \theta^t - \lambda_{\text{RMS}} \nabla L(\theta^t), \quad (15)$$

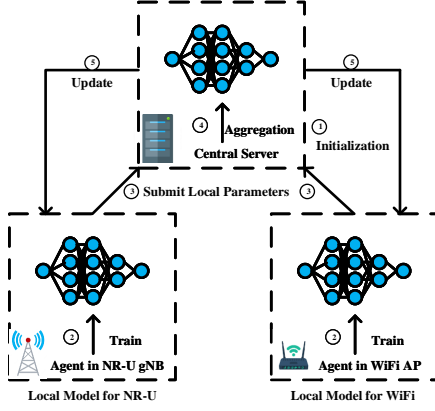


Fig. 6. Structure of federated deep reinforcement learning.

- Step 5: : The combined global parameter θ is sent back to the corresponding agents and both agents update their local models based on the received global parameters.

During training, the parameter $\tilde{\theta}_l, l = \{n, w\}$ can be updated as

$$\tilde{\theta}_l^{t+1} = \tilde{\theta}_l^t - \lambda_{\text{RMS}} \nabla L_l(\tilde{\theta}_l^t), \quad (17)$$

where $\lambda_{\text{RMS}} \in (0, 1]$ is the learning rate, $\nabla L_l(\tilde{\theta}_l^t)$ is the loss function gradient of the NR-U network or the WiFi network, which can be denoted as

$$\begin{aligned} \nabla L_l(\theta_l^t) = & \mathbb{E}_{S_l^i, A_l^i, R_l^{i+1}, S_l^{i+1}} [(R_l^{i+1} + \gamma \max_a Q(S_l^{i+1}, a; \tilde{\theta}_l^t) \\ & - Q(S_l^i, A_l^i; \tilde{\theta}_l^t)) \nabla_{\theta_l} Q(S_l^i, A_l^i; \tilde{\theta}_l^t)], \end{aligned} \quad (18)$$

where $(S_l^i, A_l^i, S_l^{i+1}, R_l^{i+1})$ are randomly selected previous samples for $i \in \{t - M_r, \dots, t\}$. $\tilde{\theta}_l$ is the target Q-network which is used to estimate the future value of the state-action value function in the update rule. In addition, the updated parameter $\tilde{\theta}_l$ will be transmitted to the central server and the model parameter θ can be updated as

$$\theta = \frac{1}{2} (\tilde{\theta}_n + \tilde{\theta}_w), \quad (19)$$

where $\tilde{\theta}_n$ and $\tilde{\theta}_w$ represent the model parameters in the NR-U and WiFi networks, respectively.

It is noted that Gate Recurrent Unit (GRU) is adopted in the proposed learning framework to approximate the value function. The complexity of GRU is calculated as $O(n_i n_l n_h^2)$, where n_i is the input size, n_l is the number of layers, and n_h is the hidden size. Without loss of generality, we assume the number of training episodes for convergence to be I , and length of each episode to be T . Therefore, the complexity of centralized-DQN and federated-DQN is $O(n_i n_l n_h^2 I T)$ and $O(X n_i n_l n_h^2 I T)$, respectively, where X is the number of agents in the federated-DQN.

V. SIMULATION

In this section, we evaluate the performance of the proposed centralized DQN and federated DQN approaches in Sec. IV via numerical experiments. We adopt the standard network

parameters listed in Table. II following [27], [29]–[31], [47]. In the following, we first present our simulation results of system throughput optimization in Section V-A, then redesign the reward function to guarantee the cell throughput of WiFi network with more dynamic Beta traffic in Section V-B.

TABLE II
SIMULATION PARAMETERS

Parameters	Value
Height of gNB and AP	3 m
Height of UE and STA	1 m
File Size	0.5 Mbytes
SIFS	16us
Defer	79us
Maximum Contention Window	1024
Packet Arrival Rate	2
Transmit Power of UE and STA	18dBm
Transmit Power of gNB and AP	23dBm
Noise Power	-104dBm
SCS	60KHz
Mini-slot	36us
Time Limitation	8s
WiFi SINR Threshold	9dB
NR-U SINR Threshold	5.5dB
WiFi Rate	21.7Mbps
NR-U Rate	25.2Mbps
WiFi COT	2.528ms
NR-U COT	6ms
WiFi Preamble Detection Threshold	-82dBm
WiFi Energy Detection Threshold	-62dBm
NR-U Energy Detection Threshold	-72dBm
Number of UEs associated with each gNB	5
Number of STAs associated with each AP	5
Simulation Length	250s

A. Uplink System Throughput Optimization

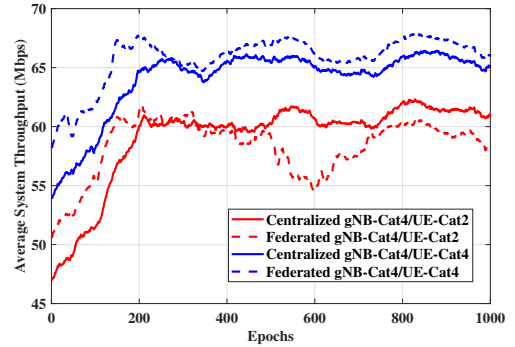


Fig. 7. Average uplink system throughput during training phase of proposed DRL algorithms.

Fig. 7 plots the average uplink system throughput during the training phase of proposed centralized and federated DRL algorithms. We can see that the average uplink system throughput of proposed centralized and federated DRL algorithms with gNB-Cat4/UE-Cat4 reaches around 65Mbps. However, the average uplink system throughput with gNB-Cat4/UE-Cat2 stabilizes only around 60Mbps. This is because the gNB has to reschedule the UE when the channel is busy during Cat2 LBT, which leads to unnecessary controlling overheads. We can also

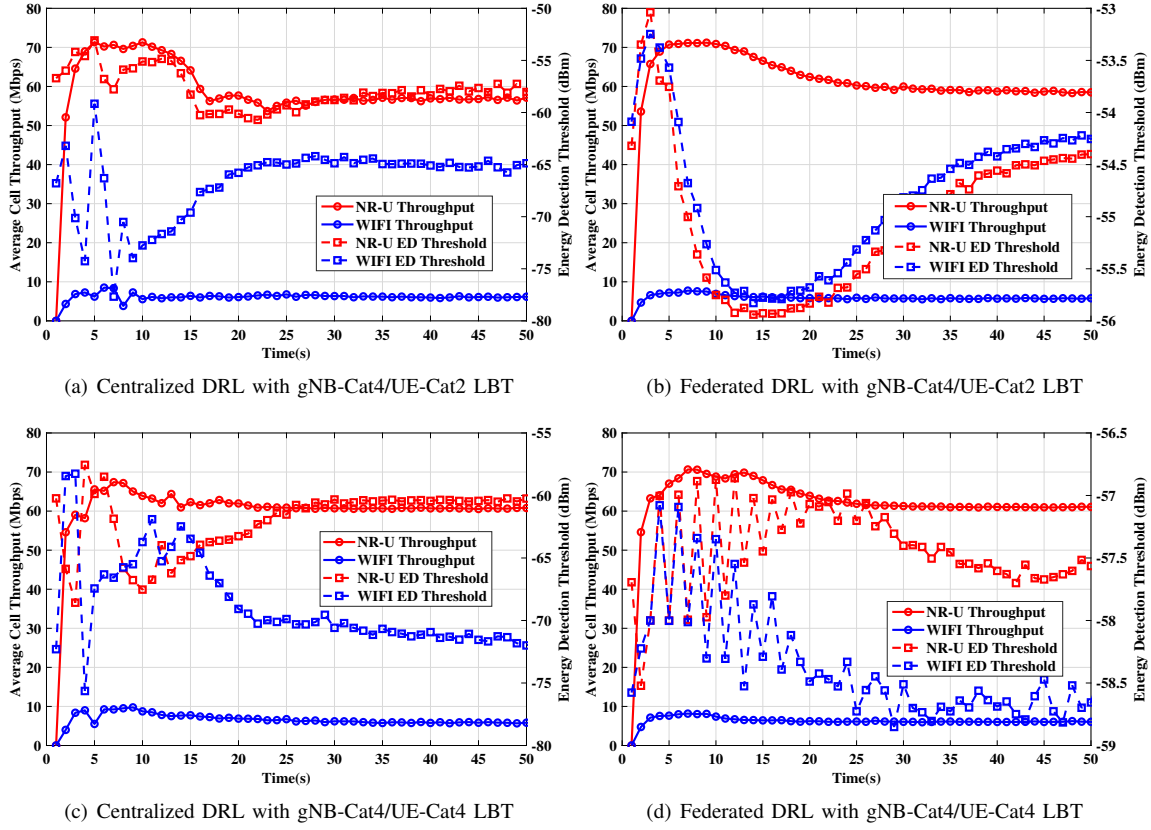


Fig. 8. Cell throughput and actions of WiFi and NR-U networks during testing phase.

observe that the federated DRL algorithms converge faster than the centralized DRL algorithms due to the much smaller action space in the setting. More importantly, centralized-DQN may easily converge to the local optimal solution due to large action space. Therefore, we can observe that the federated-DQN achieves higher performance than the centralized-DQN algorithm. However, the training phase of federated DRL algorithms is more fluctuated due to the model parameters averaging between heterogeneous networks.

As shown in Fig. 8, we test the performance of converged trained model, where the average cell throughput and ED thresholds of NR-U and WiFi networks are characterized, respectively. We can see that the networks reach the stable state around 40 seconds. This is because the traffic follows Poisson arrival with a fixed average arrival rate, and the packet that violates the time constraint is dropped.

Fig. 8 (a)(b) plot the average cell throughput and ED thresholds with gNB-Cat4/UE-Cat2 LBT scheme. In Fig. 8(a), we can observe that the cell throughput of NR-U network is around 58 Mbps, which is much higher than 6 Mbps of WiFi network. This can be explained from two aspects: 1) NR-U network has advantages over WiFi network including higher data rate, larger COT length, centralized scheduling, etc; 2) Due to the advantages of NR-U network, it can contribute more significantly to the improvement of the system throughput. Therefore, we can see that NR-U network adopts the ED threshold around -57 dBm, which is higher than the -66 dBm of WiFi network. The higher ED threshold

further enables the NR-U network to get more transmission opportunities. In Fig. 8(b), we can see that although the NR-U and WiFi networks adopt similar ED thresholds around -54 dBm, the uplink throughput of NR-U and WiFi networks are still around 58 Mbps and 6 Mbps, respectively. The reason is that there is the other CS threshold $\lambda_w^{CS} = -82\text{dBm}$, which limits the transmission of the WiFi network.

Fig. 8 (c)(d) plot the average cell throughput and ED thresholds with gNB-Cat4/UE-Cat4 LBT scheme. Compared with gNB-Cat4/UE-Cat2 LBT scheme, we can see that the NR-U network achieves higher cell throughput around 61 Mbps, while the cell throughput of WiFi network is still around 6 Mbps. This is because the gNB is required to perform the Cat4 LBT to schedule the UE again when the UE detects the channel busy during Cat2 LBT. However, if the UE performs the Cat4 LBT, the UE can adopt the Backoff procedure to wait for the transmission opportunity, which leads to less controlling overheads. We can also observe that the ED thresholds of both centralized and federated DRL algorithms are lower than that of gNB-Cat4/UE-Cat2 LBT scheme. The reason is that the gNB-Cat4/UE-Cat-4 scheme can deal with the traffic more effectively, hence, the interference level is relatively lower.

Fig. 9 plots the average cell throughput and UPT of the proposed DRL algorithms and benchmark scheme with fixed ED thresholds. In the gNB-Cat4/UE-Cat2 scheme, we can see that the cell throughput of NR-U network increases from 16 Mbps to 58 Mbps with over 250% performance gain, and the

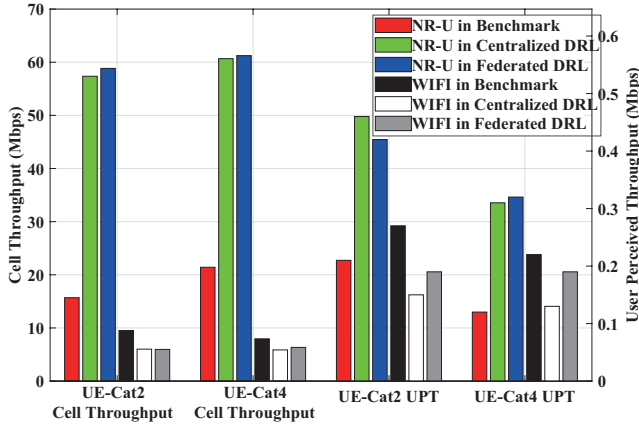


Fig. 9. Average cell throughput and user perceived throughput during testing phase.

cell throughput of WiFi network decreases from 9.5 Mbps to 6 Mbps with performance degradation around 35%. The system throughput increases from 25.5 Mbps to 64 Mbps, where the performance gain is over 150%. The performance gain of the NR-U network comes from the much higher ED threshold compared to the WiFi network as shown in Fig. 8, which indicates that the agent chooses to sacrifice the performance of WiFi network to get higher system throughput.

We can observe that the UPT of NR-U network in the benchmark is lower than that of WiFi network due to the scheduling overheads in the NR-U network. In the gNB-Cat4/UE-Cat2 scheme, the UPT of NR-U network increases from 0.21 Mbps to around 0.45 Mbps with performance gain over 100%, and UPT of WiFi network decreases from 0.27 Mbps to around 0.17 Mbps with performance degradation around 35%. This is because the NR-U network can occupy the channel to transmit the packet more timely with a higher ED threshold. It is noted that the UPT of NR-U network in federated DRL is lower than that of centralized learning. However, the UPT of WiFi network in federated DRL is higher than that of centralized learning. The reason is that both NR-U and WiFi networks adopt higher ED thresholds in federated DRL. The interference level experienced by the NR-U network reaches its decoding capability limitation due to the high ED threshold. On the contrary, the interference level experienced by the WiFi network is far away from its decoding capability limitation due to the CS threshold $\lambda_w^{CS} = -82\text{dBm}$.

In the gNB-Cat4/UE-Cat4 scheme, we can see that the cell throughput of NR-U network increases from 21 Mbps to 61 Mbps with over 180% performance gain, and the cell throughput of WiFi network decreases from 8 Mbps to 6 Mbps with performance degradation around 20%. The system throughput increases from 29 Mbps to 67 Mbps, where the performance gain is over 120%. The UPT of NR-U network increases from 0.12 Mbps to around 0.31 Mbps with performance gain over 150%, and UPT of WiFi network decreases from 0.27 Mbps to around 0.16 Mbps with performance degradation around 20%. As we discussed above, since the interference level is lower in the gNB-Cat4/UE-Cat4 scheme, we can see that the UPT of both NR-U and WiFi networks in federated DRL is higher than

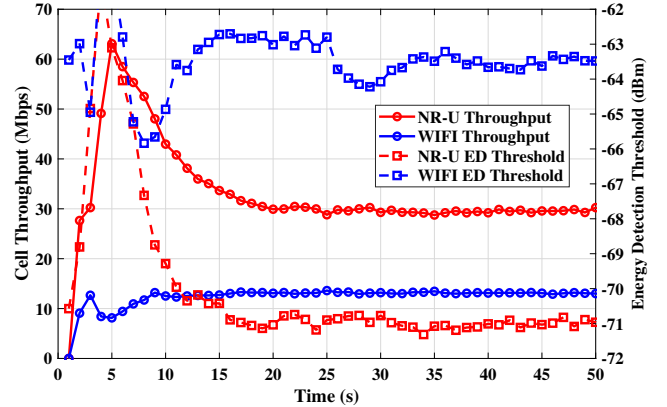
that of centralized DRL. This is because the interference with higher ED thresholds is still within the decoding capability of NR-U and WiFi devices.

B. Uplink System Throughput Optimization with Fairness

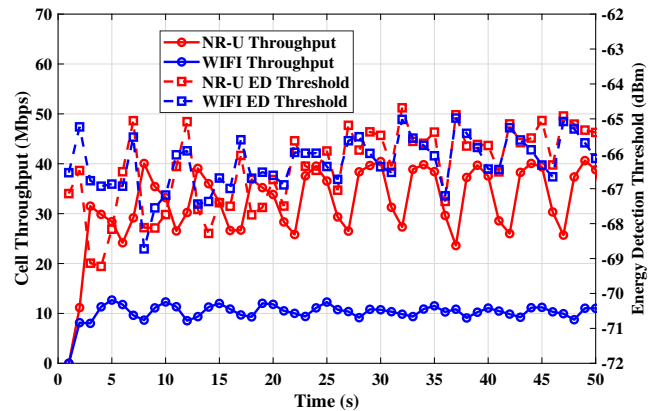
In Section V-A, the simulation results have shown that although the system throughput has been improved significantly, the agent chooses to sacrifice the cell throughput of the WiFi network to get higher cell throughput of NR-U network. To guarantee the fairness, we define the fairness as that the cell throughput of WiFi network should be higher than the pre-defined threshold. It is noted that the fairness criterion in 3GPP is a special case of proposed fairness, where the threshold is cell throughput of WiFi network under the coexistence of two WiFi networks [30]. Specifically, the reward is redesigned as

$$R^{t+1} = \begin{cases} (N_w^t + N_n^t) * S_{\text{file}} & , N_w^t * S_{\text{file}} \geq T_{\text{wifi}} \\ 0 & , N_w^t * S_{\text{file}} < T_{\text{wifi}} \end{cases} \quad (20)$$

where T_{wifi} is the pre-defined cell throughput threshold of the WiFi network. Here, the T_{wifi} is set as the cell throughput of WiFi network in the benchmark scheme with fixed ED thresholds. As the FTP-3 traffic follows Poisson arrival with fixed arrival rate, we further verify the proposed DRL algorithm with more dynamic Beta traffic [48].



(a) gNB-Cat4/UE-Cat2 LBT with FTP-3 traffic



(b) gNB-Cat4/UE-Cat2 LBT with Beta traffic

Fig. 10. Cell throughput and actions of WiFi and NR-U networks during testing phase.

As shown in the Fig. 10, we test the performance of converged trained model, where the average cell throughput and ED thresholds of NR-U and WiFi networks are characterized, respectively. We can see that the networks reach the stable state around 40 seconds under FTP-3 traffic, but the networks dynamically change over time under Beta traffic. Under FTP-3 traffic in the Fig. 10(a), we can see that the cell throughput of NR-U network stabilizes around 31 Mbps, which is lower compared to the 58 Mbps in Fig. 8. However, the cell throughput of WiFi network stabilizes around 13 Mbps, which is higher than the 6 Mbps in Fig. 8. This can be explained that the NR-U network adopts -71 dBm ED threshold, but WiFi network adopts a higher ED threshold around -64 dBm. Under Beta traffic in the Fig. 10(b), we can observe that the ED thresholds of NR-U and WiFi networks have a similar dynamic range from -65 dBm to -67 dBm. However, the cell throughput dynamic range of NR-U network is much larger than that of WiFi network. This is because the fixed -82 dBm CS threshold limits the transmission of WiFi network.

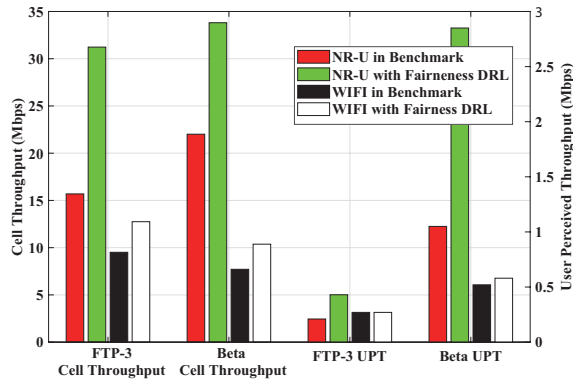


Fig. 11. Average cell throughput and user perceived throughput during testing phase in gNB-Cat4/UE-Cat2 scheme.

Fig. 11 plots the average cell throughput and UPT of the proposed DRL algorithm with a re-designed reward function and benchmark scheme with fixed ED thresholds. Overall, we can see that the cell throughput of WiFi network is not sacrificed while improving the system throughput. Under FTP-3 traffic, we can see that the cell throughput of NR-U network increases from 16 Mbps to 31 Mbps with around 100% performance gain, and the cell throughput of WiFi network increases from 9.5 Mbps to 13 Mbps with performance gain over 35%. The system throughput increases from 25.5 Mbps to 44 Mbps, where the performance gain is over 70%. The performance gain of the system throughput decreases compared to the algorithm without considering the fairness due to the lower ED threshold in NR-U network, which indicates the effectiveness of the re-designed reward. We can observe that the UPT of NR-U network increases from 0.21 Mbps to around 0.43 Mbps with performance gain over 100%, which shows the re-designed reward has little influence on the UPT of NR-U network. However, UPT of WiFi network remains around 0.27 Mbps, which is a large improvement compared to the result without fairness. Under Beta traffic, we can see that the cell throughput performance gain of NR-U and WiFi

networks are around 50%, and 30%, respectively, which leads to the system throughput gain around 48%.

VI. CONCLUSION AND FUTURE WORK

In this paper, we developed a novel centralized DRL framework and a federated DRL framework, respectively, to optimize the ED thresholds configuration for maximizing the uplink system throughput in UCBC under the coexistence of heterogeneous NR-U and WiFi networks. We first developed a centralized double Deep Q-Network (DDQN) algorithm for the dynamic ED thresholds configuration with an agent deployed at the central server, where two different uplink transmission schemes (i.e., gNB-Cat4/UE-Cat2 and gNB-Cat4/UE-Cat4) are considered. To protect the data privacy, we further developed a federated DDQN algorithm to dynamically optimize the ED thresholds for NR-U and WiFi networks, where two independent agents are deployed in the heterogeneous NR-U and WiFi networks and only exchange the model parameters with the central server, respectively. Furthermore, we re-designed the reward function to guide the agent to guarantee the cell throughput of WiFi network while improving the uplink system throughput, where the agent gets punished when the cell throughput of WiFi network is below the pre-defined threshold. Finally, we introduced a user-centric performance metric called UPT to evaluate the file transmission throughput from the perspective of users.

Our results demonstrated that our proposed DRL-based ED thresholds configuration approaches significantly outperform the benchmark scheme in terms of both uplink system throughput and UPT. Our numerical results shed light on that the NR-U network has inherent advantages over the WiFi network, including the data rate, MCOT length, scheduling policy, etc, which makes the fairness among heterogeneous networks to be an important problem to study.

REFERENCES

- [1] F. Hu, Y. Deng, H. Zhou, T. H. Jung, C.-B. Chae, and A. H. Aghvami, "A vision of an XR-aided teleoperation system toward 5G/B5G," *IEEE Commun. Mag.*, vol. 59, no. 1, pp. 34–40, Jan. 2021.
- [2] H. Zhou, C. She, Y. Deng, M. Dohler, and A. Nallanathan, "Machine learning for massive industrial internet of things," *IEEE Wireless Commun.*, vol. 28, no. 4, pp. 81–87, Aug. 2021.
- [3] K. B. Letaief, Y. Shi, J. Lu, and J. Lu, "Edge artificial intelligence for 6G: Vision, enabling technologies, and applications," *IEEE J. Sel. Areas Commun.*, vol. 40, no. 1, pp. 5–36, Jan. 2022.
- [4] *Huawei 5.5G*. [Online]. Available: <https://www.huawei.com/en/news/2020/11/mbbf-shanghai-huawei-david-wang-5dot5g>
- [5] A. Mukherjee, J.-F. Cheng, S. Falahati, H. Koorapaty, D. H. Kang, R. Karaki, L. Falconetti, and D. Larsson, "Licensed-Assisted Access LTE: coexistence with IEEE 802.11 and the evolution toward 5G," *IEEE Commun. Mag.*, vol. 54, no. 6, pp. 50–57, Jun. 2016.
- [6] H.-J. Kwon, J. Jeon, A. Bhorkar, Q. Ye, H. Harada, Y. Jiang, L. Liu, S. Nagata, B. L. Ng, T. Novlan, J. Oh, and W. Yi, "Licensed-assisted access to unlicensed spectrum in LTE Release 13," *IEEE Commun. Mag.*, vol. 55, no. 2, pp. 201–207, Feb. 2017.
- [7] Q. Chen, G. Yu, and Z. Ding, "Enhanced LAA for unlicensed LTE deployment based on TXOP contention," *IEEE Trans. Commun.*, vol. 67, no. 1, pp. 417–429, Jan. 2019.
- [8] M. Hirzallah, M. Krunz, B. Kecioglu, and B. Hamzeh, "5G new radio unlicensed: Challenges and evaluation," *IEEE Trans. on Cogn. Commun. Netw.*, vol. 7, no. 3, pp. 689–701, Sep. 2021.
- [9] S. Lagen, L. Giupponi, S. Goyal, N. Patriciello, B. Bojović, A. Demir, and M. Beluri, "New radio beam-based access to unlicensed spectrum: Design challenges and solutions," *IEEE Commun. Surveys Tuts.*, vol. 22, no. 1, pp. 8–37, 1st Quart., 2020.

- [10] G. Naik, J.-M. Park, J. Ashdown, and W. Lehr, "Next generation Wi-Fi and 5G NR-U in the 6 GHz bands: Opportunities and challenges," *IEEE Access*, vol. 8, pp. 153 027–153 056, 2020.
- [11] G. Bianchi, "Performance analysis of the IEEE 802.11 distributed coordination function," *IEEE J. Sel. Areas Commun.*, vol. 18, no. 3, pp. 535–547, Mar. 2000.
- [12] J. Tan, S. Xiao, S. Han, Y.-C. Liang, and V. C. M. Leung, "Qos-aware user association and resource allocation in LAA-LTE/WiFi coexistence systems," *IEEE Trans. Wireless Commun.*, vol. 18, no. 4, pp. 2415–2430, Apr. 2019.
- [13] H. Bao, Y. Huo, X. Dong, and C. Huang, "Joint time and power allocation for 5G NR unlicensed systems," *IEEE Trans. Wireless Commun.*, vol. 20, no. 9, pp. 6195–6209, Sep. 2021.
- [14] S. Liu, R. Yin, and G. Yu, "Hybrid adaptive channel access for LTE-U systems," *IEEE Trans. Veh. Technol.*, vol. 68, no. 10, pp. 9820–9832, Oct. 2019.
- [15] J. Peng, Y. Gao, X. Sun, W. Zhan, and Z. Guo, "3GPP fairness constrained throughput optimization for 5G NR-U and WiFi coexistence in the unlicensed spectrum," in *Proc. IEEE Wireless Commun. Netw. Conf.*, Apr. 2022, pp. 1779–1784.
- [16] A. Daraseliya, M. Korshykov, E. Sopin, D. Moltchanov, S. Andreev, and K. Samouylov, "Coexistence analysis of 5G NR Unlicensed and WiGig in millimeter-wave spectrum," *IEEE Trans. Veh. Technol.*, vol. 70, no. 11, pp. 11 721–11 735, Nov. 2021.
- [17] N. Jiang, Y. Deng, and A. Nallanathan, "Traffic prediction and random access control optimization: Learning and non-learning-based approaches," *IEEE Commun. Mag.*, vol. 59, no. 3, pp. 16–22, Mar. 2021.
- [18] L. Zhang, H. Yin, Z. Zhou, S. Roy, and Y. Sun, "Enhancing WiFi multiple access performance with federated deep reinforcement learning," in *2020 IEEE 92nd Vehicular Technology Conference (VTC2020-Fall)*, IEEE, Nov. 2020, pp. 1–6.
- [19] U. Challita, L. Dong, and W. Saad, "Proactive resource management for LTE in unlicensed spectrum: A deep learning perspective," *IEEE Trans. Wireless Commun.*, vol. 17, no. 7, pp. 4674–4689, Jul. 2018.
- [20] J. Tan, L. Zhang, Y.-C. Liang, and D. Niyato, "Intelligent sharing for LTE and WiFi systems in unlicensed bands: A deep reinforcement learning approach," *IEEE Trans. Commun.*, vol. 68, no. 5, pp. 2793–2808, May 2020.
- [21] J. Tan, S. Xiao, S. Han, and Y.-C. Liang, "A learning-based coexistence mechanism for LAA-LTE based hetnets," in *2018 IEEE International Conference on Communications (ICC)*, IEEE, May 2018, pp. 1–6.
- [22] R. Ali, Y. B. Zikria, S. Garg, A. K. Bashir, M. S. Obaidat, and H. S. Kim, "A federated reinforcement learning framework for incumbent technologies in beyond 5G networks," *IEEE Netw.*, vol. 35, no. 4, pp. 152–159, Jul. 2021.
- [23] Z. Ali, L. Giupponi, J. Mangues-Bafalluy, and B. Bojovic, "Machine learning based scheme for contention window size adaptation in LTE-LAA," in *2017 IEEE 28th Annual International Symposium on Personal, Indoor, and Mobile Radio Communications (PIMRC)*, IEEE, Oct. 2017, pp. 1–7.
- [24] E. Pei, Y. Huang, L. Zhang, Y. Li, and J. Zhang, "Intelligent access to unlicensed spectrum: a mean field based deep reinforcement learning approach," *IEEE Trans. Wireless Commun.*, vol. 22, no. 4, pp. 2325 – 2337, Apr. 2022.
- [25] A. K. Bairagi, S. F. Abedin, N. H. Tran, D. Niyato, and C. S. Hong, "QoE-enabled unlicensed spectrum sharing in 5G: A game-theoretic approach," *IEEE Access*, vol. 6, pp. 50 538–50 554, 2018.
- [26] A. K. Bairagi, N. H. Tran, W. Saad, Z. Han, and C. S. Hong, "A game-theoretic approach for fair coexistence between LTE-U and Wi-Fi systems," *IEEE Trans. Veh. Technol.*, vol. 68, no. 1, pp. 442–455, 2019.
- [27] *Study on NR-based access to unlicensed spectrum*, document TR 38.889 V16.0.0, 3GPP, Sophia, Antipolis, France, 2018.
- [28] B. McMahan, E. Moore, D. Ramage, S. Hampson, and B. A. y Arcas, "Communication-efficient learning of deep networks from decentralized data," in *Artificial intelligence and statistics*. PMLR, 2017, pp. 1273–1282.
- [29] *Study on channel model for frequencies from 0.5 to 100 GHz*, document TR 38.901 V16.1.0, 3GPP, Sophia, Antipolis, France, 2019.
- [30] *Study on Licensed-Assisted Access to Unlicensed Spectrum*, document TR 36.889 V13.0.0, 3GPP, Sophia, Antipolis, France, 2015.
- [31] *Further advancements for E-UTRA physical layer aspects*, document TR 36.814 V9.2.0, 3GPP, Sophia, Antipolis, France, 2017.
- [32] Q.-D. Ho, D. Tweed, and T. Le-Ngoc, *Long Term Evolution in Unlicensed Bands*, 2017.
- [33] V. Loginov, E. Khorov, A. Lyakhov, and I. Akyildiz, "Cr-lbt: Listen-before-talk with collision resolution for 5G NR-U networks," *IEEE Trans. Mobile Comput.*, pp. 1–1, [early access] 2021.
- [34] J. Kim, J. Yi, and S. Bahk, "Uplink channel access enhancement for cellular communication in unlicensed spectrum," *IEEE Access*, vol. 8, pp. 216 386–216 397, 2020.
- [35] K. Kosek-Szott, A. Lo Valvo, S. Szott, P. Gallo, and I. Tinnirello, "Downlink channel access performance of NR-U: Impact of numerology and mini-slots on coexistence with Wi-Fi in the 5 GHz band," *Comm Com Inf Sc*, vol. 195, p. 108188, Aug. 2021.
- [36] J. Zheng, J. Xiao, Q. Ren, and Y. Zhang, "Performance modeling of an LTE LAA and WiFi coexistence system using the LAA Category-4 LBT procedure and 802.11e EDCA mechanism," *IEEE Trans. Veh. Technol.*, vol. 69, no. 6, pp. 6603–6618, Jun. 2020.
- [37] Y. Ma, "Analysis of channel access priority classes in lte-laa spectrum sharing system," in *2018 27th International Conference on Computer Communication and Networks (ICCCN)*. IEEE, Jul. 2018, pp. 1–7.
- [38] X. Sun and L. Dai, "Towards fair and efficient spectrum sharing between LTE and WiFi in unlicensed bands: Fairness-constrained throughput maximization," *IEEE Trans. Wireless Commun.*, vol. 19, no. 4, pp. 2713–2727, Apr. 2020.
- [39] M. Mehrnough, V. Sathya, S. Roy, and M. Ghosh, "Analytical modeling of Wi-Fi and LTE-LAA coexistence: Throughput and impact of energy detection threshold," *IEEE/ACM Trans. Netw.*, vol. 26, no. 4, pp. 1990–2003, Aug. 2018.
- [40] C. S. Yang, C. K. Kim, J.-M. Moon, S.-H. Park, and C. G. Kang, "Channel access scheme with alignment reference interval adaptation (aria) for frequency reuse in unlicensed band LTE: Fuzzy Q-Learning approach," *IEEE Access*, vol. 6, pp. 26 438–26 451, 2018.
- [41] R. S. Sutton and A. G. Barto, *Reinforcement Learning: An Introduction*, 2018.
- [42] N. Jiang, Y. Deng, A. Nallanathan, and J. A. Chambers, "Reinforcement learning for real-time optimization in NB-IoT networks," *IEEE J. Sel. Areas Commun.*, vol. 37, no. 6, pp. 1424–1440, Jun. 2019.
- [43] N. Jiang, Y. Deng, A. Nallanathan, and J. Yuan, "A decoupled learning strategy for massive access optimization in cellular IoT networks," *IEEE J. Sel. Areas Commun.*, vol. 39, no. 3, pp. 668–685, Mar. 2021.
- [44] Y. Liu, Y. Deng, M. ElKashlan, A. Nallanathan, and G. K. Karagiannidis, "Optimization of grant-free NOMA with multiple configured-grants for mURLLC," *IEEE J. Sel. Areas Commun.*, vol. 40, no. 4, pp. 1222–1236, Apr. 2022.
- [45] H. Van Hasselt, A. Guez, and D. Silver, "Deep reinforcement learning with double q-learning," in *Proceedings of the AAAI conference on artificial intelligence*, vol. 30, no. 1, Mar. 2016.
- [46] T. Sylla, L. Mendiboure, S. Maaloul, H. Aniss, M. A. Chalouf, and S. Delbruel, "Multi-connectivity for 5G networks and beyond: A survey," *Sensors*, vol. 22, no. 19, p. 7591, Oct. 2022.
- [47] L. Li, J. P. Seymour, L. J. Cimini, and C.-C. Shen, "Coexistence of Wi-Fi and LAA networks with adaptive energy detection," *IEEE Trans. Veh. Technol.*, vol. 66, no. 11, pp. 10 384–10 393, Nov. 2017.
- [48] J. Navarro-Ortiz, P. Romero-Diaz, S. Sendra, P. Ameigeiras, J. J. Ramos-Munoz, and J. M. Lopez-Soler, "A survey on 5G usage scenarios and traffic models," *IEEE Commun. Surveys Tuts.*, vol. 22, no. 2, pp. 905–929, 2nd Quarter., 2020.